

# Determining Slope Stability by Rigid Finite Element Method and Limit Analysis Methods

Amir Mohammad Merati<sup>1\*</sup>, Hasan Ghasemzadeh<sup>2</sup> and Seyyed Mohammad Farid Astaneh<sup>3</sup>

1- MSc in Soil Mechanics & foundation

2- Associate prof. at K.N.Toosi University of Technology

3- Assistant prof. at Islamic Azad University, Central Tehran Branch

*Corresponding author:* Amir Mohammad Merati

**ABSTRACT:** The analysis of soil slopes stability is an issue being analyzed using various methods such as limit equilibrium and its relevant software. In this paper, limit equilibrium method based on plasticity theory has been used. In this paper, Based on upper and lower bound limit theorem and using principle of virtual work for calculations, the authors will introduce an overturning failure criterion to govern both the kinematically and statically admissible fields in the limit analysis and overall factor of safety of slopes stability is introduced at the end of this research. This research utilizes rigid finite element method considering the rotating-sliding mechanism. The results comparisons of the current research with previous ones show considerable results.

**Keywords:** Slope stability, Limit analysis, Plasticity, Rigid finite element method, Linear programming.

## INTRODUCTION

The Finite Element Method (FEM) based on limit analysis is a conventional method in analyzing the limit state issues for various researchers. An obvious drawback with the traditional FEM-based limit analysis approaches being applied to rock slopes is their inability to characterize the behavior of discontinuous rock masses. In this regard, a good alternative would be the rigid FEM. RFEM is inspired by a technique called Rigid Body Spring Model (RFSM) introduced in 1977. (1)

With a lower degree of freedom for the elements considered in the RFEM than that in the traditional FEM, the computational efficiency may be much improved. Importantly, the physical discontinuities in discontinuous media can be reasonably treated as interfaces between the adjacent rigid elements in RFEM. (2)

In RFEM, The pre-process of data and the process of analysis is same as conventional FEM but the difference is that the main 2 items in RFEM are "Elements" and "Interface", whereas the main items in FEM are "Elements" and "Mesh". In this method, each element is considered Rigid. the study area has been meshed in a way that connects each element via interface. Displacements in each point of the rigid element are related to rotational and translational movements of the center of element.

In RFEM, the displacements occurred in the center of elements are our main variables, whereas the main variables in conventional FEM are displacements in domain nodes.

Despite the Gauss Stress Tensor method in traditional FEM, the stress-strain analysis of the forces at the element's interface is calculated with a different method in a way that while using Mohr-Coulomb failure condition, the normal and shear forces over each interface are directly affecting failure. In fact, it is assumed that the interfaces between rigid elements may be our failures surfaces which result in the calculations being so sensitive to dimension and mesh design of the domain. (3)

### **Assumption for Numerical Discretization Based on Rigid Finite Elements**

The following assumptions are generally taken in a RFEM:

- All elements are assumed to be rigid and are connected to one another by the element interface.

- The deformation energy of a system is stored in the interfaces only, and a discontinuous velocity field is allowed at the interface.
- The interfaces are assumed to be isotropic, and their deformation is perfectly plastic, obeying the Mohr Coulomb yield condition and the associated flow rule. With these

Assumptions, the “compatibility” and “equilibrium equations” between rigid elements can be found as follows: (2)

**Compatibility Equation of Discontinuous Kinematical Admissible Velocity Field**

In previous RFEM-based limit studies, the constraints of compatibility were considered in a way that rotation had been ignored in the center of the elements. In a research done by Liu & Zhao, (2013) (2), the constraints of compatibility has been revised in a way that rotational velocity  $\dot{\omega}$  is used in the compatibility equation based on mathematical solution of toppling proposed by Goodman and Bray (1981). (4)

The discontinuous kinematically admissible velocity between two adjacent rigid elements in a typical upper bound analysis can now develop into two failure modes, namely, the simple sliding failure, which is controlled by the Mohr-Coulomb criterion, and the rotational failure, which is controlled by the new overturning criterion. A possible discontinuous kinematical admissible velocity field at the interface is shown in Fig. 1 where  $P_m$  denotes the center of the  $k$ -th interface between two typical rigid elements  $i$  and  $j$ . The discontinuous velocity can be conveniently measured by a strain rate vector as follows:

$$\dot{\epsilon}_k = [\dot{n}_k \quad \dot{s}_k \quad \dot{\theta}_k]^T \tag{1}$$

where  $\dot{n}_k$ ,  $\dot{s}_k$  and  $\dot{\theta}_k$  = relative tangential, normal, and angular displacement rates, at the center of the joint, respectively. (2)

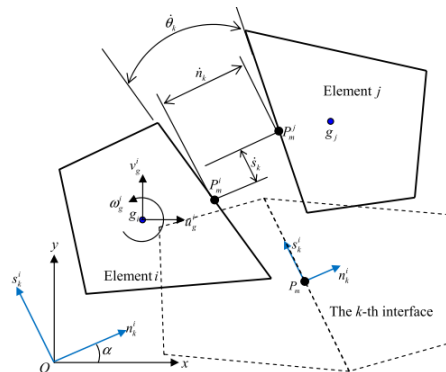


Figure 1. Kinematically admissible discontinuous velocity field of interface between two rigid elements

The discontinuous strain rate vectors at all interfaces of a discretized RFEM domain can be assembled into the following vector:

$$\dot{\epsilon}^T = [\dot{\epsilon}_1^T, \dots, \dot{\epsilon}_{n_d}^T]^T \tag{2}$$

where  $n_d$  = number of all interfaces.

In local coordinates  $s_k^i$ - $o$ -  $n_k^i$ , the velocity at the center  $P_m$  of the  $k$ th interface caused by the centroid velocity of  $i$ th element can be written as:

$$\dot{\epsilon}_{i/k} = L_{i/k} N_{i/k} \dot{u}_i \tag{3}$$

Where in the vector below:

$$\dot{u}_i = [\dot{u}_g^i \quad \dot{v}_g^i \quad \dot{\omega}_g^i] \tag{4}$$

$u_i$  = centroid velocity of the  $i$ th element;  $u_g^i$  and  $v_g^i$  = translational velocities in the x-and y-directions of the global coordinates x-o-y;  $\omega_g^i$  = rotational velocity of the  $i$ th element.  $N_{i/k}$  = RFEM shape function of the  $i$ th element corresponding to the  $k$ th interface; and  $L_{i/k}$  = matrix of direction cosines of the local  $s_k^i$ - $o$ -  $n_k^i$  axes for the  $k$ th interface with respect to the global coordinate system x-o-y. Specifically,  $N_{i/k}$  &  $L_{i/k}$  are formulated as follows:



$N_k$ , and the moment  $M_k$ , all applied at the center of the interface as shown in Fig. 2. They can be denoted in a vector form as: (12)

$$Q_k = [ N_k \quad V_k \quad M_k ]^T, k=1, \dots, n_d \tag{15}$$

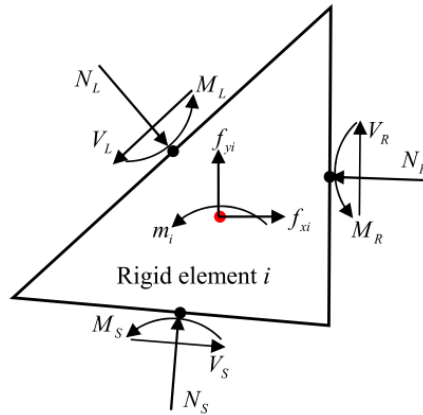


Figure 2. Forces acting on one rigid finite element

The global stress vector can be written collectively as follows (formula 16):

$$Q^T = [ Q_1^T \quad Q_2^T \quad \dots \quad Q_{n_d}^T ] \tag{16}$$

According to the principle of virtual work, in a equilibrium system the external force along with the virtual displacement equals to internal energy waste. In RFEM, the energy for changing the form of system is stored between interfaces of the elements. There would be no stress occurred in rigid element and consequently there would be no energy waste inside the element. Therefore, the equation of principle of virtual work would be:

$$- \delta \dot{\epsilon}^T Q - \delta \dot{U}^T \cdot \lambda F = 0 \tag{17}$$

Substitution of Eq. (13) into Eq. (17) leads to:

$$- \delta \dot{U}^T B^T Q - \lambda \delta \dot{U}^T F = 0 \tag{18}$$

Considering  $\partial \dot{U} \neq 0$  in general cases gives the following global equilibrium equation:

$$- B^T Q - \lambda F = 0 \tag{19}$$

Where:

$$F^T = [ f_1^T \quad f_2^T \quad \dots \quad f_m^T ] \tag{20}$$

$$f_m = [ f_{xi} \quad f_{yi} \quad m_i ]^T \tag{21}$$

(21) Represents global external force vector to the  $i$ -th component. This equilibrium is the same as the one proposed by Ferris and Tin-Loi (2001). (3)

**Yield Criteria and Flow Rules for Sliding and Rotation Mechanisms**

The kinematical admissible discontinuous velocity derived in the Equilibrium Equations for Rigid Element section can be separated into two failure modes, namely, relative sliding and rotation of an element with respect to its adjacent element.

Accordingly, two different yield conditions are employed to govern the failures at the interface: a Mohr-Coulomb criterion for the sliding failure and an overturning failure criterion for the rotation failure.

**Sliding Mechanism between Two Rigid Elements**

Fig. (1), illustrates a translational sliding of element j over element i. Mobilization of this translational mechanism may be described by the Mohr-Coulomb criterion, i.e.

$$|\tau| = c + \tan \varphi \sigma_n \tag{21}$$

Note that compression is taken to be positive here. Based on the generalized stress defined in Eq. (11), the above Mohr-Coulomb failure criterion may be recast to the following form:

$$|V_k| - \tan \varphi N_k - c \Delta x = 0 \tag{22}$$

where  $\Delta x$  = total length of interface. Note that the use of the absolute value of  $V_k$  indicates that the shear direction is unrestricted.

**Rotational Failure Mechanism between Two Rigid Elements**

Element rotation has been ignored by previous RFEM-based limit analyses by other researchers and the main purpose was to maintain the condition of no gap or overlap between neighboring elements. Although it appears to be reasonable for the translation-dominant type of slope failure, the assumption proves to be inadequate to describe cases (such as upwelling underground water or increase in the height of soil slopes) where the rotation may be a contributing factor. The criterion is generalized based on the toppling failure criterion originally proposed by Goodman and Bray (1981). Consider a block on an inclined surface subjected to self-weight only (Fig. 3). Fig. 3 shows a state in which a rotation or toppling of the block is pending. The critical condition can be expressed as:

$$\frac{y}{\Delta x} \leq \cot \alpha \tag{23}$$

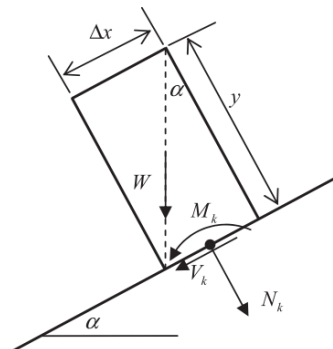


Figure 3. Failure criterion by block toppling

By multiplying both sides of the inequality in Eq. (24) with the weight W of the block, the following expression of the failure criterion is obtained:

$$M_k - N_k \frac{\Delta x_k}{2} \leq 0, \quad M_k = \frac{W \cdot \sin \alpha \cdot y}{2}, \quad N_k = W \cdot \cos \alpha \tag{24}$$

To facilitate the subsequent numerical implementation, the sliding failure criterion and the overturning failure criterion for the  $k$ -th interface can be collectively expressed in the following matrix form:

$$\phi_k = \Phi_k^T Q_k + a_k \leq 0, \Phi_k^T = \begin{bmatrix} -\tan \varphi_k & 1 & 0 \\ -\tan \varphi_k & -1 & 0 \\ \frac{-\Delta x}{2} & 0 & 1 \\ \frac{-\Delta x}{2} & 0 & -1 \end{bmatrix}, a_k = \begin{bmatrix} -c_k \Delta x_k \\ -c_k \Delta x_k \\ 0 \\ 0 \end{bmatrix} \quad (25)$$

Where  $\varphi_k$  and  $c_k$  = friction angle and cohesion at the  $k$ -th interface, respectively. The failure criteria at all interfaces can then be assembled in the following matrix formulation:

$$\begin{aligned} \phi &= \Phi^T Q + a \leq 0 \\ \phi^T &= \left[ \phi_1^T \quad \phi_2^T \quad \dots \quad \phi_{n_d}^T \right]_{(1 \times 4n_d)} \\ \Phi^T &= \begin{pmatrix} \Phi_1^T & 0 & \dots & 0 \\ 0 & \Phi_2^T & & 0 \\ \vdots & 0 & \ddots & 0 \\ 0 & 0 & 0 & \Phi_{n_d}^T \end{pmatrix}_{(4n_d \times 3n_d)} \\ a^T &= \left[ a_1^T \quad a_2^T \quad \dots \quad a_{n_d}^T \right] \end{aligned} \quad (26)$$

Where  $n_d$  = number of interfaces in the discretized domain.

**Associated Flow Rule**

In conjunction with the previously given failure criteria, additional constraints on the kinematically admissible velocity field are needed by considering the associated flow rule. For interface sliding, the associated flow rule assumes that the tangential velocity change,  $\dot{\mu}$ , is accompanied by the separation velocity,  $\dot{\mu} \tan \varphi$  (Fig. 4). As for the interface overturning, the associated flow rule requires that the normal velocity change  $\dot{\mu}$  corresponds to an opening angle change of  $2\dot{\mu} / \Delta x$  (Fig. 4).

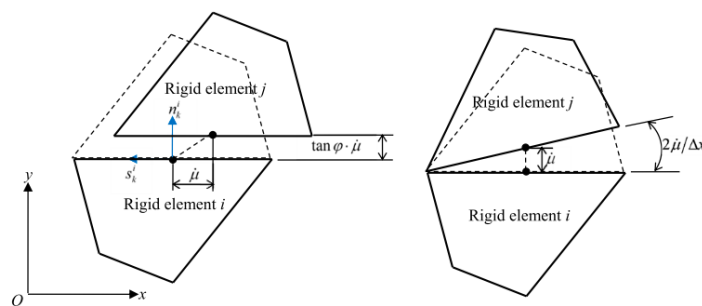


Figure 4. Sliding & Rotational Interface Failure modes between two rigid elements

In relation to the velocity vector in Eq. (1), these kinematic slip and rotation conditions can be expressed as Eq. (27):

$$\dot{\epsilon}_i = - \dot{\mu}_k \cdot \partial \phi_k / \partial Q_i \tag{27}$$

Assembling all the associated flow equations for the interface gives:

$$\dot{\epsilon}_k = - \Phi_k \dot{\mu}_k \tag{28}$$

In Eq. (28),  $\dot{\mu}_k$  vector is written as:

$$\dot{\mu}_k = \left[ \mu_{1k}, \mu_{2k}, \mu_{3k}, \mu_{4k} \right]^T \tag{29}$$

Where  $\dot{\mu}_k$  = vector of nonnegative plastic multipliers. By substituting Eq. (28) into  $\dot{\epsilon} = B\dot{U}$ , the compatibility condition can be reformulated as follows:

$$B \dot{U} = -\Phi \dot{\mu} \tag{30}$$

With previously given compatibility equation and equilibrium equation, the upper and lower bound limit analysis can be treated as a unified mathematical programming problem, which will be conducted in the Linear Programming for RFEM-Based Limit Analysis section. (2)

**Linear Programming for RFEM-Based Limit Analysis**

As shown previously, the kinematically admissible velocity field has been separated into sliding and rotational modes, and the relative rotation between two rigid elements is governed by the toppling failure criterion in Eq. (24). Following the assumption of the associated flow rule, the relative rotation is further introduced into the governing equations of the kinematically and statically admissible fields in the limit analysis. In addition, the compatibility, equilibrium, and failure equations formulated previously are all in linear form. Taking this feature, the authors can then formulate the upper and lower bound theorems into a dual of two linear programming problems.(5)

**Primal Problem of Linear Programming for Kinematic Approach**

The upper bound approach of limit theory states that any limit load multiplier  $\lambda$  for a kinematically admissible velocity restricted by the compatibility equation and associated flow rule, i.e., Eq. (30), cannot be smaller than the plastic collapse multiplier  $\lambda_c$ , i.e.,  $\lambda \leq \lambda_c$ . An upper bound limit analysis aims to find the minimum of the load multiplier  $\lambda_{min}$  to approximate  $\lambda_c$ . Using the associated flow rule in Eq. (28) in the virtual principle in Eq. (17) gives the following equation for the load multiplier:

$$\dot{\mu}^T \Phi^T Q - \lambda \dot{U}^T F = 0 \tag{31}$$

Further substitution of the failure criteria in Eq. (27) into the previously revised virtual principle, leads to Eq. (34):

By  $\dot{\mu}^T (\phi - a) - \lambda \dot{U}^T F = 0 \tag{32}$

considering the complementary condition  $\dot{\mu}^T \phi = 0$ , the load multiplier can be formulated as follows:

$$\lambda = -\dot{\mu}^T a, \text{ When } \dots \dot{U}^T F = 1 \tag{33}$$

As a result, the upper bound approach can be formulated as the following linear programming problem Eq. (34):

$$\min(\lambda) = -\dot{\mu}^T a \quad s.t. \begin{cases} \dot{U}^T F = 1 \\ B\dot{U} = -\Phi\dot{\mu}, \quad 0 \leq \dot{\mu} \end{cases} \tag{34}$$

Notethat boundary conditions in the upper bound approach constitute mainly prescribed velocities, for example,  $\dot{U} = 0$ . Although they do not contribute to the real velocity field, the generalized primal variables in Eq. (34) will not include the quantities on the prescribed boundaries.

**Dual Problem for Static Approach**

In the lower bound approach of limit theory, any load multiplier  $\lambda$  corresponding to a statically admissible stress field constrained by the equilibrium equation and the failure criteria cannot be greater than the plastic collapse multiplier  $\lambda_c$ , i.e.,  $\lambda \leq \lambda_c$ . The linear programming problem of a lower bound approach is to find the maximum of the load multiplier  $\lambda_{max}$ . Alternatively, according to the dual theory of linear programming, the lower bound approach can be also formulated as the following dual of the primal problem of the corresponding upper bound approach:

$$\max(\lambda) \quad st \begin{cases} -B^T Q - \lambda F = 0 \\ \phi = \Phi^T Q + a \leq 0 \end{cases} \quad (35)$$

According to the duality theory of linear programming, the upper (primal) and the lower (dual) bound solutions can be found by solving the following optimal (Karush- Kuhn-Tucker (KKT)) conditions utilized in MOSEK (7) package:

$$\begin{bmatrix} 0 & 0 & F & 0 \\ 0 & 0 & B & \Phi \\ -F & -B^T & 0 & 0 \\ 0 & -\Phi^T & 0 & 0 \end{bmatrix} \begin{bmatrix} \lambda \\ Q \\ \dot{U} \\ \dot{\mu} \end{bmatrix} + \begin{bmatrix} 0 \\ 0 \\ 0 \\ -\phi \end{bmatrix} = \begin{bmatrix} 1 \\ 0 \\ 0 \\ -a \end{bmatrix} \quad where \begin{cases} \phi^T \dot{\mu} = 0 \\ 0 \leq \dot{\mu} \\ \phi \leq 0 \end{cases} \quad (36)$$

The matrix contains  $\lambda, Q, \dot{U}, \dot{\mu}$  parameters which represent limit load multiplier, stress between elements, velocity of element and plastic multipliers respectively. To solve the matrix above, the boundary conditions and bound solutions must be satisfied by defining appropriate upper and lower limits for the unknowns in the matrix prior to solving the problem.

**Satisfying the boundary conditions**

In solving the problem, we satisfy the boundary conditions by assuming the upper and lower boundaries of velocity parameters of stability elements as zero. Therefore, the programming and enhancement techniques are being implemented and optimum limit load multiplier  $\lambda$  and other velocity parameters are calculated.

**Evaluating the stability of soil slope**

In previous sections, the formulation applied during the various phases of the research is comprehensively described. In this section, the problem and the edited algorithm is being evaluated using the programming algorithm used by Liu & Zhao, (2013) (2).

The problem is a soil slope with three different soil layers. The shear strength parameters and unit weight of each layer are also summarized in Table 1. The domain is discretized by an unstructured triangle mesh as shown in Fig. 5. (6)

Table 1. Shear Strength Parameters and Unit Weights of Soils

Soil Layer	C (kN/m <sup>2</sup> )	$\phi$ (degree)	$\gamma$ (kN/m <sup>3</sup> )
1	294	40	18.8
2	9.8	5	18.8
3	29.4	12	18.8

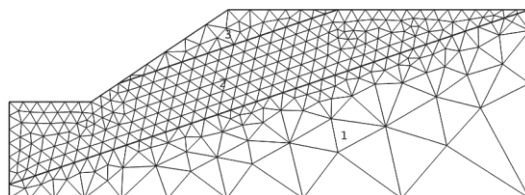


Figure 5. Typical rigid finite-element mesh for the inhomogeneous slope using COSMOL software



The method of reducing strength has been employed to find the factor of safety for this problem, by following the common definition of the factor of safety:

$$F_s = \frac{c'}{c'_m} = \frac{\tan \varphi'}{\tan \varphi'_m} \tag{37}$$

Where  $c'$  and  $\varphi'$  = effective cohesion and internal frictional angle, respectively; and  $c'_m$  and  $\varphi'_m$  = reduced (mobilized) cohesion and frictional angle, respectively.

The factor of safety  $F_s$  is computed in conjunction with optimization of the limit load multiplier  $\lambda$  according to Eq. (36). Specifically, an initial value  $F_s$  (usually a small one) is chosen first to calculate the reduced cohesion and frictional angle  $c'_m$  and  $\varphi'_m$  according to Eq. (37). These two strength parameters are substituted into Eq. (26) to obtain an optimal limit load multiplier  $\lambda$  using the proposed method and MOSEK software. The process is repeated by gradually increasing the value of the factor of safety from its initial value. Consequently, a series of limit load multipliers in conjunction with the corresponding factor of safety can be obtained, which can be plotted in a figure like Fig. 6. The ultimate factor of safety for the problem corresponds to the value at the intersection of the curve with the horizontal line  $\lambda = 1$ .

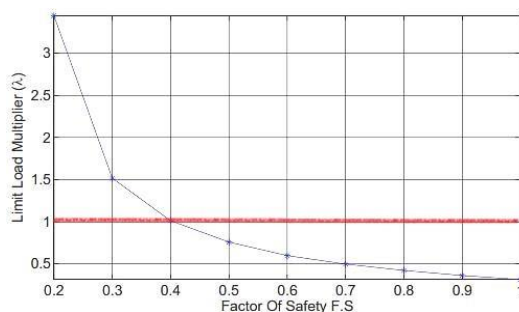


Figure 9. Determination of the factor of safety by optimizing limit loading multiplier

As is summarized in Table 2, in particular, the factor of safety in consideration for both sliding and rotation failure modes is found between the upper bound and lower bound obtained in this research and is compared with the results obtained by Spencer’s method along with the results obtained by (Liu & Zhao, 2013) (2).

Table 2. Comparison of Factor of Safety by Various Methods

Authors	Methods	$F_s$
Present method	Spencer’s method	0.41
Present method	Janbu method	0.38
Present method	Limit Analysis (LimitState:GEO)	0.47
Present method	RFEM-based limit analysis	0.405
Liu & Zhao, 2013	RFEM-based limit analysis	0.421

As the table shows, the obtained factor of safety from RFEM-based limit analysis methods is in the range of other methods. The resulted algorithm (with 4% variation) has an appropriate conformity with Liu & Zhao (2013) results.

Fig. (7) shows Kinematically admissible velocity fields. the arrows show the direction of velocity vectors in the model.

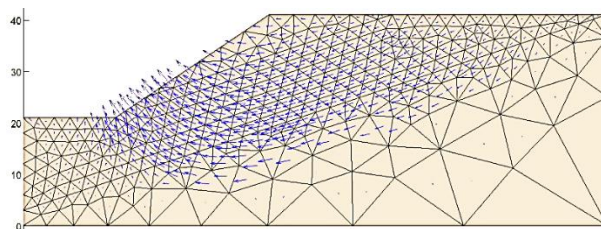


Figure 7. Kinematically admissible velocity fields obtained Limit Analysis

Fig. (8) shows the sliding line obtained from SLOPE/W in comparison with LimitState:GEO. The dashed line is the result of SLOPE/W software and the solid line for LimitState:GEO.

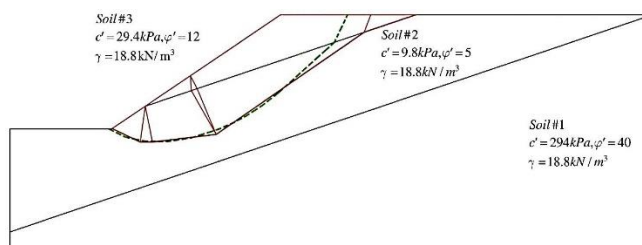


Figure 8. Comparison of Sliding line results of SLOPE/W & LimitState:GEO for the inhomogeneous slope problem

The failure line obtained by LimitState:GEO software (solid line) shows that the soil slope at the upper part of Soil #2 (middle layer) has more penetration and consequently, is close to the result of SLOPE/W software. But in other parts, these 2 results are close to each other. Meanwhile, the failure lines of Janbu, Spencer and other methods are all close to the dashed line in Fig. (8).

**Implementing sensitivity analysis on parameters**

For all the Analysis performed in this section, the variation of Factor of safety against the changes of geometrical parameters such as angle of slope and height of the block for the Soil #3 (Table.1) are being assessed. Also, the variation of Factor of safety against mechanical parameters changes of the soil such as internal friction angle and soil cohesion (when the internal friction angle is constant) is being evaluated. For comparison, Janbu method has been used in order to analyze the results by SLOPE/W software.

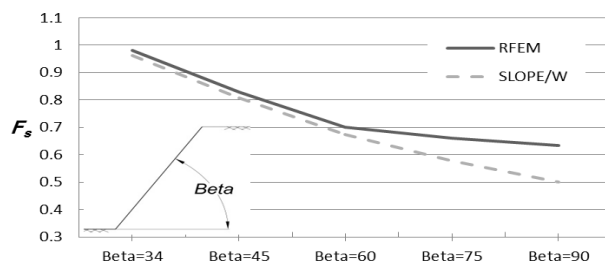


Figure 9. Changes of Factor of Safety versus slope angle changes

The results show that the Factor of Safety difference (variance) in 2 above method is 2% from Angle 34° to 60°. The variance increases as the slope angle goes beyond 60°.

Fig. (10), shows the changes in soil cohesion and its effect on Factor of safety. The results show that the difference of  $F_s$  amounts in the two compared methods widens as the soil cohesion increases.

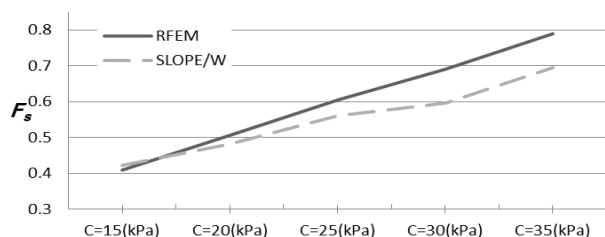


Figure 10. Changes of Factor of Safety versus soil cohesion (with constant internal friction angle)

**Conclusion and results of the introduced method**

Based on the RFEM, a general formulation of upper and lower bound limit analysis has been presented. The upper and lower bound solution is expressed as primal and dual linear programming problems that can be solved by an efficient and robust primal-dual interior-point method. This method proved that it may be used to solve problems

in large scale and numerous elements. One of the issues in solving this problem was the non-convergence of Factor of safety results. Better defining the Matrix of direction cosines and better meshing was very effective in solving the problem correctly. Future study will focus on the enhancing Rotational failure criterion and its improvement for being used in rock slopes.

## REFERENCES

- Cheng YM and Lau CK. 2008. "*Slope Stability Analysis and Stabilization*". USA, Routledge.
- Fentago L and Jidong Z. 2013. "Limit Analysis of Slope Stability By Rigid Finite Element Method And Linear Programming Considering Rotational Failure". Int. J. Geomechanics, ASCE.
- Ferris MC and Tin-Loi F. 2001. "*Limit Analysis of Frictional Block Assemblies as a Mathematical Program with Complementarity Constraints*", Int. J. Mechanical Sciences.
- Goodman RE and Bray JW . 1981. "*The theory of base friction models*". Int. J. Rock Mech. Min. Sci. & Geomec.
- Kim J, Salgado R and Lee J. 2002. "*Stability Analysis of Complex Soil Slopes using Limit Analysis*". *Journal Of Geotechnical And Geoenvironmental Engineering*, ASCE.
- MOSEK. 2012. "*The MOSEK optimization toolbox for MATLAB manual. Version 7.0*" Copenhagen, Denmark, MOSEK ApS.
- Roos. 2005. "*Interior Point Methods for Linear Optimization*", USA, Springer.